Event-Based Kalman Filtering Exploiting Correlated Trigger Information

Benjamin Noack[1], Clemens Öhl[2], and Uwe D. Hanebeck[2]

[1]*Autonomous Multisensor Systems Group*
Institute for Intelligent Cooperating Systems
Otto von Guericke University Magdeburg
Magdeburg, Germany
benjamin.noack@ieee.org

[2]*Intelligent Sensor-Actuator-Systems Laboratory (ISAS)*
Institute for Anthropomatics and Robotics
Karlsruhe Institute of Technology (KIT)
Karlsruhe, Germany
clemens.oehl@alumni.kit.edu, uwe.hanebeck@ieee.org

***Abstract*—In networked estimation architectures, event-based sensing and communication can contribute to a more efficient resource allocation in general, and improved utilization of communication resources, in particular. In order to tap the full potential of event-based scheduling, the design of transmission triggers and estimators need to be closely coupled while two directions are promising: First, the remote estimator can exploit the absence of transmissions and translate it into implicit information about the sensor data. Second, an intelligent trigger mechanism at the sensor that predicts future sensor readings can decrease transmission rates while rendering the implicit information more valuable. Such an intelligent trigger has been developed in a recent paper based on a Finite Impulse Response filter, which requires the sensor to transmit an additional estimate alongside the measurement. In the present paper, the communication demand is further reduced by only transmitting the estimate. The remote estimator exploits correlations to incorporate the received information. In doing so, the estimation quality is also improved, which is confirmed by simulations.**

***Index Terms*—Event-based estimation, finite impulse response filter, stochastic triggering**

I. Introduction

Networked estimation is key to leveraging recent advances of sensor, communication, and processing technologies. Sensor data can be acquired ubiquitously and pervasively, e.g., by wireless sensor networks [1], [2], the Internet-of-Things [3], vehicular networks [4], or crowd sensing [5]. Distributed estimation [6], [7] enables an in-network processing of the accrued sensor data. Despite its advantages over centralized processing architectures, distributed estimation brings a number of additional challenges that have been addressed by a variety of different approaches [8], [9]. Particular attention has been directed towards correlations [10], [11] between the estimates of different network nodes. Attaining optimal estimation results is only possible under strict assumptions on network topology, communication rates, and computational resources. Examples include distributed formulations of the Kalman filter equations or augmented state representations [12]–[14] with some relaxations, e.g., in [15], [16]. For optimal fusion, methods to keep track of correlations have been introduced in [17] or [18]. Suboptimal fusion methods follow a different direction, for which covariance intersection [19], [20] with its further developments [21]–[23] is the most prominent solution.

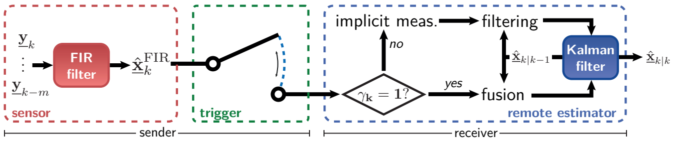

Fig. 1: Scheme of proposed event-based filtering

From an estimation point of view, networked sensor systems should send as much data as often as possible. However, resource efficiency becomes a major concern, in particular, in battery-driven systems, and some resources like a shared communication channel cannot be accessed at all times. For this reason, greater attention is being devoted to finding trade-offs between estimation quality and resource utilization in networked sensor–estimator systems. To reduce the amount of data, measurements and estimates can be quantized [24], [25] without violating their consistency, or the most informative parts can be selected [26]. To reduce the communication rate, one can shift away from periodic transmission schedules to data-driven transmissions [27]–[29]. Such event-based mechanisms find particular application in networked control systems [30], [31] and typically employ a trigger at the sensor to decide for a transmission. Variance-based triggers [32], [33] or send-on-delta schemes [34] are prominent examples of such mechanisms. The design of the trigger is crucial to finding a trade-off between communication rate and estimation quality. Finding good trade-offs can be addressed at two places: At the sensor, an intelligent trigger can further reduce the transmission rate by predicting the system behavior to assess the measurement's contribution to the remote estimate. At the remote estimator, the absence of a transmission still carries useful information about the sensor data if the estimator knows the trigger's decision rule. The estimator still infers information about the actual measurement—called implicit or negative information—to perform a measurement update. For deterministic triggers, negative information refers to set-membership measurement representations, which have been exploited in different works [35]–[38] using a hybrid estimator [39]. Another approach that is also followed by this paper rests upon stochastic trigger mechanisms [40], which preserve the Gaussianity of the implicit information. In doing so, the remote estimator can be a standard Kalman filter with only minor adaptions, which renders stochastic triggering particularly appealing for distributed Kalman filtering. Examples are the information [41] and consensus [42] filter using stochastic triggers, which also include triggering on input information [43].

In this paper, we will further investigate event-based estimation with Gaussianity-preserving triggers that are reviewed in Sec. III. As shown in our previous work [44], stochastic triggers integrate well with intelligent prediction mechanisms at the sensors. There, the sensor runs a Finite Impulse Response (FIR) filter [45] in parallel to predict future measurements and compares them with the actual sensor data to decide for a transmission. The trigger inherits the advantageous properties of the FIR filter e.g., no prior information is required, and robustness against outliers is increased. The sensor, in particular, becomes more resilient in the presence of unmodeled errors. This approach also shows that the trigger can be designed independently of the remote estimator. However, as described in Sec. IV, solutions using estimate-based triggers have the drawback that the sensor has to send both measurements and the estimate, where the latter is required by the remote estimator to compute the implicit information. In Sec. V, we will show how a remote estimator can be designed that only uses the FIR estimate and fuses it optimally with its own Kalman estimate by exploiting correlations, which is illustrated in Fig. 1. This approach not only reduces the data to be communicated but also increases the remote estimation quality, which is confirmed by the simulations in Sec. VI. Sec. VII discusses the results and outlines possible extensions of this work.

II. Notation

An underlined variable $\underline{x} \in \mathbb{R}^n$ denotes a real-valued vector. Lowercase boldface letters $\underline{\mathbf{x}}$ are used for random quantities. Matrices are written in uppercase boldface letters $\mathbf{C} \in \mathbb{R}^{n \times n}$, and $\mathbf{C}^{-1}$ and $\mathbf{C}^{\mathrm{T}}$ are its inverse and transpose, respectively. $\mathbf{0}_{m \times n}$ is the zero matrix with m rows and n columns. $\mathbf{0}_m \in \mathbb{R}^{m \times m}$ or $\mathbf{I}_m \in \mathbb{R}^{m \times m}$ are the zero or identity square matrices, respectively. The notation $\hat{\underline{\mathbf{x}}}_k^{\mathrm{FIR}}$ is used for an FIR estimate; $\hat{\underline{\mathbf{x}}}_{k|k}$ denotes an estimate of a Kalman filter.

III. Gaussianity-Preserving Triggering

This section introduces the models and concepts used throughout this paper and gives an overview of Gaussianity-preserving trigger designs.

A. System Model & State Estimation

Discrete-time linear system and measurement models are considered, which are governed by

$$\begin{aligned} \underline{\mathbf{x}}_{k+1} &= \mathbf{A}_k \, \underline{\mathbf{x}}_k + \underline{\mathbf{w}}_k \ , \\ \underline{\mathbf{y}}_k &= \mathbf{C}_k \, \underline{\mathbf{x}}_k + \underline{\mathbf{v}}_k \ , \end{aligned} \tag{1}$$

where $\underline{\mathbf{x}}_k \in \mathbb{R}^{n_x}$ is the state at time step $k \in \mathbb{N}$, and $\underline{\mathbf{y}}_k \in \mathbb{R}^{n_y}$ denotes the observation. The time-variant process and measurement matrices are given by $\mathbf{A}_k \in \mathbb{R}^{n_x \times n_x}$ and $\mathbf{C}_k \in \mathbb{R}^{n_y \times n_x}$, respectively. The process noise $\underline{\mathbf{w}}_m \sim \mathcal{N}(\underline{0}, \mathbf{Q})$ and measurement noise $\underline{\mathbf{v}}_n \sim \mathcal{N}(\underline{0}, \mathbf{R})$ are white and mutually uncorrelated for arbitrary $m, n \in \mathbb{N}$.

To estimate the state, a discrete-time Kalman filter is considered. It is initialized with the prior estimate $\hat{\underline{\mathbf{x}}}_{0|0} \in \mathbb{R}^{n_x}$ and covariance matrix $\mathbf{P}_{0|0} \in \mathbb{R}^{n_x \times n_x}$. The time update or prediction step yields

$$\hat{\underline{\mathbf{x}}}_{k+1|k} = \mathbf{A}_k \, \hat{\underline{\mathbf{x}}}_{k|k} \ , \tag{2}$$

$$\mathbf{P}_{k+1|k} = \mathbf{A}_k \, \mathbf{P}_{k|k} \, \mathbf{A}_k^{\mathrm{T}} + \mathbf{Q} \ , \tag{3}$$

where $\mathbf{P}_{k+1|k}$ is the covariance of the estimation error $\hat{\underline{\mathbf{x}}}_{k+1|k} - \underline{\mathbf{x}}_{k+1}$. The measurement update using the observation $\underline{\mathbf{y}}_k$ is obtained by

$$\hat{\underline{\mathbf{x}}}_{k|k} = \hat{\underline{\mathbf{x}}}_{k|k-1} + \mathbf{K}_k \left(\underline{\mathbf{y}}_k - \mathbf{C}_k \, \hat{\underline{\mathbf{x}}}_{k|k-1} \right) \ , \tag{4}$$

$$\mathbf{P}_{k|k} = \left(\mathbf{I}_{n_x} - \mathbf{K}_k \, \mathbf{C}_k \right) \mathbf{P}_{k|k-1} \ , \tag{5}$$

$$\mathbf{K}_k = \mathbf{P}_{k|k-1} \, \mathbf{C}_k^{\mathrm{T}} \Big(\mathbf{C}_k \mathbf{P}_{k|k-1} \, \mathbf{C}_k^{\mathrm{T}} + \mathbf{R} \Big)^{-1} \ , \tag{6}$$

where $\mathbf{K}_k$ is the Kalman gain. The zero-mean error $\hat{\underline{\mathbf{x}}}_{k|k} - \underline{\mathbf{x}}_k$ has the covariance matrix $\mathbf{P}_{k|k}$.

B. Stochastic Triggering

Let $\underline{\mathbf{y}}_k \in \mathbb{R}^{n_y}$ represent the sensor data for which a trigger decision is to be made. The variable $\gamma_k = 1$ denotes that an event is triggered, and $\underline{\mathbf{y}}_k$ is sent to the receiver. For $\gamma_k = 0$, no transmission is triggered. To determine γ_k, an independently and identically distributed random variable $\boldsymbol{\xi}_k$ is generated that is uniformly distributed over $[0, 1]$. The decision scheme is given by

$$\gamma_k = \begin{cases} 1, & \boldsymbol{\xi}_k > \phi(\underline{\mathbf{y}}_k - \underline{c}_k) \, , \\ 0, & \boldsymbol{\xi}_k \leq \phi(\underline{\mathbf{y}}_k - \underline{c}_k) \, , \end{cases} \tag{7}$$

with $\phi(\underline{\mathbf{y}}_k - \underline{c}_k) = \exp\Big(-\frac{1}{2} \, (\underline{\mathbf{y}}_k - \underline{c}_k)^{\mathrm{T}} \, \mathbf{Z}_k^{-1} \, (\underline{\mathbf{y}}_k - \underline{c}_k) \Big)$ to compare $\underline{\mathbf{y}}_k$ against a chosen $\underline{c}_k \in \mathbb{R}^{n_y}$. The matrix $\mathbf{Z}_k \in \mathbb{R}^{n_y \times n_y}$ is a design parameter to tune the transmission rate. Due to the design of $\phi(\cdot)$ and the properties of $\boldsymbol{\xi}_k$, the transmission probability given $\underline{\mathbf{y}}_k$ yields

$$\begin{aligned} \Pr\big\{ \gamma_k = 1 \, \big| \, \underline{\mathbf{y}}_k \big\} &= 1 - \phi(\underline{\mathbf{y}}_k - \underline{c}_k) \, , \\ \Pr\big\{ \gamma_k = 0 \, \big| \, \underline{\mathbf{y}}_k \big\} &= \phi(\underline{\mathbf{y}}_k - \underline{c}_k) \, . \end{aligned} \tag{8}$$

The likelihood $\Pr\big\{ \gamma_k = 0 \, \big| \, \underline{\mathbf{y}}_k \big\}$ is exploited in the following to infer information about $\underline{\mathbf{y}}_k$ when the sensor does not trigger a transmission.

IV. Event-Based Kalman Filtering With FIR-Based Triggers

A predictive trigger design has been proposed in our earlier publication [44], which equips the sensor with an FIR filter to predict sensor readings. These predictions are fed as decision variable $\underline{c}_k$ into the trigger (7). This section briefly discusses the FIR-based trigger mechanism and shows yet to be improved properties.

A. FIR-Based Stochastic Triggering and Estimation

The sensor employs an advanced trigger by employing a local FIR-based estimator as, e.g., described in [45]. For this purpose, a horizon of $(m+1)$ time steps is considered, and the acquired measurements are described by the stacked equation

$$\underline{\mathbf{y}}_{\text{last}} = \boldsymbol{\mathcal{H}}_k \cdot \underline{\mathbf{x}}_k + \underline{\mathbf{n}}_k \tag{9}$$

with

$$\underline{\mathbf{y}}_{\text{last}} := \begin{bmatrix} \underline{\mathbf{y}}_k \\ \underline{\mathbf{y}}_{k-1} \\ \vdots \\ \underline{\mathbf{y}}_{k-m} \end{bmatrix}, \quad \boldsymbol{\mathcal{H}}_k := \begin{bmatrix} \mathbf{C}_k \\ \mathbf{C}_{k-1}\,(\boldsymbol{\mathcal{A}}_{k-1}^{k-1})^{-1} \\ \vdots \\ \mathbf{C}_{k-m}\,(\boldsymbol{\mathcal{A}}_{k-1}^{k-m})^{-1} \end{bmatrix},$$

and $\boldsymbol{\mathcal{A}}_i^j := \mathbf{A}_i \cdot \mathbf{A}_{i-1} \cdot \ldots \cdot \mathbf{A}_j$. Hence, the collected measurements are expressed with respect to $\underline{\mathbf{x}}_k$. The horizon $(m+1)$ must be chosen large enough so that $\boldsymbol{\mathcal{H}}_k$ has full column rank. For the noise $\underline{\mathbf{n}}_k$, we study the measurement $\underline{\mathbf{y}}_{k-l}$ for $l \in \{1, \ldots, m\}$ and its corresponding row in (9), which yields

$$\begin{aligned} \underline{\mathbf{y}}_{k-l} &= \mathbf{C}_{k-l}\underline{\mathbf{x}}_{k-l} + \underline{\mathbf{v}}_{k-l} \\ &= \mathbf{C}_{k-l}\mathbf{A}_{k-l}^{-1}\big(\underline{\mathbf{x}}_{k-l+1} - \underline{\mathbf{w}}_{k-l}\big) + \underline{\mathbf{v}}_{k-l} = \ldots \\ &= \mathbf{C}_{k-l}\big(\boldsymbol{\mathcal{A}}_{k-1}^{k-l}\big)^{-1}\underline{\mathbf{x}}_k - \sum_{i=1}^{l} \mathbf{C}_{k-l}\big(\boldsymbol{\mathcal{A}}_{k-i}^{k-l}\big)^{-1}\underline{\mathbf{w}}_{k-i} + \underline{\mathbf{v}}_{k-l}\,. \end{aligned}$$

From this equation, we can deduce the form of the vector $\underline{\mathbf{n}}_k$ in (9), which summarizes the accumulated process and measurement noise terms. It is hence given by

$$\underline{\mathbf{n}}_k = -\begin{bmatrix} \mathbf{0} \\ \mathbf{C}_{k-1}\big(\boldsymbol{\mathcal{A}}_{k-1}^{k-1}\big)^{-1}\underline{\mathbf{w}}_{k-1} \\ \vdots \\ \sum_{i=1}^{m} \mathbf{C}_{k-m}\big(\boldsymbol{\mathcal{A}}_{k-i}^{k-m}\big)^{-1}\underline{\mathbf{w}}_{k-i} \end{bmatrix} + \begin{bmatrix} \underline{\mathbf{v}}_k \\ \underline{\mathbf{v}}_{k-1} \\ \vdots \\ \underline{\mathbf{v}}_{k-m} \end{bmatrix}$$

and is zero mean with non-singular covariance matrix

$$\mathbf{V}_k = \mathrm{Cov}\{\underline{\mathbf{n}}_k\}\ .$$

The block entries have the form

$$\begin{aligned} (\mathbf{V}_k)_{(p+1)(q+1)} = &\mathbf{C}_{k-p}\left(\sum_{i=1}^{\min(p,q)}\big(\boldsymbol{\mathcal{A}}_{k-i}^{k-p}\big)^{-1}\mathbf{Q}\big(\boldsymbol{\mathcal{A}}_{k-i}^{k-q}\big)^{-\mathrm{T}}\right)\mathbf{C}_{k-q}^{\mathrm{T}} \\ &+ \delta_{pq}\mathbf{R}\,, \end{aligned}$$

where δ_{pq} is the Kronecker delta with $p, q \in \{0, 1, \ldots, m\}$ and the expression $\sum_{i=1}^{0}$ results in $\mathbf{0}$. The joint covariance matrix $\mathbf{V}_k$ characterizes the correlations between subsequent measurements due to process and measurement noise. With these equations, an uncertainty-aware FIR filter can be derived that yields

$$\hat{\underline{\mathbf{x}}}_k^{\mathrm{FIR}} = \big(\boldsymbol{\mathcal{H}}_k^{\mathrm{T}}\,\mathbf{V}_k^{-1}\,\boldsymbol{\mathcal{H}}_k\big)^{-1}\,\boldsymbol{\mathcal{H}}_k^{\mathrm{T}}\,\mathbf{V}_k^{-1}\,\underline{\mathbf{y}}_{\text{last}}\,. \tag{10}$$

Like the Kalman filter estimate, the FIR estimate $\hat{\underline{\mathbf{x}}}_k^{\mathrm{FIR}}$ is unbiased [45] with the error

$$\tilde{\underline{\boldsymbol{x}}}_k^{\mathrm{FIR}} = \hat{\underline{\mathbf{x}}}_k^{\mathrm{FIR}} - \underline{\mathbf{x}}_k = \big(\boldsymbol{\mathcal{H}}_k^{\mathrm{T}}\,\mathbf{V}_k^{-1}\,\boldsymbol{\mathcal{H}}_k\big)^{-1}\,\boldsymbol{\mathcal{H}}_k^{\mathrm{T}}\,\mathbf{V}_k^{-1}\underline{\mathbf{n}}_k \tag{11}$$

and the corresponding error covariance matrix

$$\mathbf{E} = \mathrm{Cov}\left\{\tilde{\underline{\boldsymbol{x}}}_k^{\mathrm{FIR}}\right\} = \big(\boldsymbol{\mathcal{H}}_k^{\mathrm{T}}\,\mathbf{V}_k^{-1}\,\boldsymbol{\mathcal{H}}_k\big)^{-1}\,.$$

For the event-based estimator proposed [44], the sensor sends both the measurement $\underline{\mathbf{y}}_k$ and the estimate $\tilde{\underline{\mathbf{x}}}_k^{\mathrm{FIR}}$ to the remote estimator if a transmission event is triggered. Sensor and estimator operate as follows.

1) Sensor: Given the FIR estimate $\hat{\underline{\mathbf{x}}}_{k-1}^{\mathrm{FIR}}$ from the previous time step and the current sensor reading $\underline{\mathbf{y}}_k$, the trigger mechanism first computes the predicted measurement

$$\hat{\underline{\mathbf{y}}}_k^{\mathrm{FIR}} = \mathbf{C}_k\,\mathbf{A}_{k-1}\,\hat{\underline{\mathbf{x}}}_{k-1}^{\mathrm{FIR}} \tag{12}$$

and uses $\phi(\underline{\mathbf{y}}_k - \hat{\underline{\mathbf{y}}}_k^{\mathrm{FIR}})$ in (7) to obtain γ_k and decide whether to transmit sensor information. Hence, the trigger variable $\underline{c}_k$ is set to $\hat{\underline{\mathbf{y}}}_k^{\mathrm{FIR}}$. The following two cases need to be considered:

a) $\gamma_k = 1$: In case of a transmission, the sensor computes a new FIR estimate $\hat{\underline{\mathbf{x}}}_k^{\mathrm{FIR}}$ by means of eq. (10) using the current and its buffered measurements. The current measurement and the new FIR estimate are sent to the receiver.

b) $\gamma_k = 0$: No transmission is triggered. The sensor computes a predicted FIR estimate $\hat{\underline{\mathbf{x}}}_k^{\mathrm{FIR}} = \mathbf{A}_{k-1}\,\hat{\underline{\mathbf{x}}}_{k-1}^{\mathrm{FIR}}$ for the next time step. Hence, no transmissions imply that the local FIR estimate is not updated with the recent measurements and only predicted.

In the following time step $k+1$, these steps are repeated with $\phi(\underline{\mathbf{y}}_{k+1} - \hat{\underline{\mathbf{y}}}_{k+1}^{\mathrm{FIR}})$ and $\hat{\underline{\mathbf{y}}}_{k+1}^{\mathrm{FIR}} = \mathbf{C}_{k+1}\,\mathbf{A}_k\,\hat{\underline{\mathbf{x}}}_k^{\mathrm{FIR}}$. To compute the FIR estimates, the sensor keeps a buffer of $(m+1)$ measurements. The matrix $\mathbf{Z}_k$ is a design parameter determining a trade-off between transmission rate and estimation quality.

2) Estimator: The remote estimator either receives a new measurement or deduces implicit measurement information from the absence of a transmission. For the latter, we assume a reliable communication channel so that the trigger decision is solely responsible for not sending. There are also studies on channel models including packet delays and losses that lead to more complicated estimator designs, which are not used here. The remote Kalman filter computes an estimate based on the received measurements with small modifications to the formulas in Sec. III-A. Besides the measurements $\underline{\mathbf{y}}_k$, the remote estimator receives the FIR estimate $\hat{\underline{\mathbf{x}}}_k^{\mathrm{FIR}}$ from the sensor. For the prediction step, the remote Kalman filter uses the standard equations (2) and (3). Additionally, $\hat{\underline{\mathbf{x}}}_k^{\mathrm{FIR}} = \mathbf{A}_{k-1}\,\hat{\underline{\mathbf{x}}}_{k-1}^{\mathrm{FIR}}$ is computed with the goal of keeping the FIR estimate at the sensor and remote estimator synchronized. The measurement update depends on the transmission decision:

a) $\gamma_k = 1$: In case of a transmission, the estimator receives a new measurement $\underline{\mathbf{y}}_k$ from the sensor and performs the update according to the standard formulas (4) and (5) with Kalman gain (6). The local FIR estimate is replaced with the received FIR estimate from the sensor to keep both synchronized.

b) $\gamma_k = 0$: The estimator does not receive the actual measurement and translates the absence into implicit measurement information. It makes use of the stochastic trigger (7) and its corresponding likelihood (8). As described in [40] or [44], the likelihood for $\gamma_k = 0$ given the state $\underline{\mathbf{x}}_k$ becomes

$$\begin{aligned}\Pr\{\gamma_k = 0 \,|\, \underline{\mathbf{x}}_k\} &= \int_{\mathbb{R}^{n_y}} \Pr\left\{\gamma_k = 0 | \underline{\mathbf{y}}_k, \underline{\mathbf{x}}_k\right\} \cdot \Pr\left\{\underline{\mathbf{y}}_k | \underline{\mathbf{x}}_k\right\} \mathrm{d}\underline{\mathbf{y}}_k \\ &= \int_{\mathbb{R}^{n_y}} \phi(\underline{\mathbf{y}}_k - \underline{c}_k) \cdot Pr\left\{\underline{\mathbf{y}}_k \,|\, \underline{\mathbf{x}}_k\right\} \mathrm{d}\underline{\mathbf{y}}_k \\ &\propto \exp\left(-\tfrac{1}{2}(\underline{c}_k - \mathbf{C}_k\,\underline{\mathbf{x}}_k)^{\mathrm{T}}(\mathbf{Z}_k + \mathbf{R})^{-1}(\underline{c}_k - \mathbf{C}_k\,\underline{\mathbf{x}}_k)\right)\end{aligned}$$

and preserves its Gaussianity. By comparing this to the density representation of the Kalman filter, the implicit measurement is $\underline{c}_k$ and has the covariance matrix $(\mathbf{Z}_k + \mathbf{R})$. The sensor uses $\underline{c}_k = \hat{\underline{\mathbf{y}}}_k^{\mathrm{FIR}}$ from (12), which states the reason why the remote estimator needs a copy of the FIR estimate $\hat{\underline{\mathbf{x}}}_k^{\mathrm{FIR}}$. The remote Kalman filter can now update its estimate according to

$$\begin{aligned}\hat{\underline{\mathbf{x}}}_{k|k} &= \hat{\underline{\mathbf{x}}}_{k|k-1} + \mathbf{K}_k\left(\hat{\underline{\mathbf{y}}}_k^{\mathrm{FIR}} - \mathbf{C}_k\,\hat{\underline{\mathbf{x}}}_{k|k-1}\right) , \\ \mathbf{P}_{k|k} &= \left(\mathbf{I}_{n_x} - \mathbf{K}_k\,\mathbf{C}_k\right)\mathbf{P}_{k|k-1} , \\ \mathbf{K}_k &= \mathbf{P}_{k|k-1}\,\mathbf{C}_k^{\mathrm{T}}\left(\mathbf{C}_k\mathbf{P}_{k|k-1}\,\mathbf{C}_k^{\mathrm{T}} + \mathbf{Z}_k + \mathbf{R}\right)^{-1}\end{aligned} \tag{13}$$

with the implicit measurement $\hat{\underline{\mathbf{y}}}_k^{\mathrm{FIR}}$ and an increased measurement covariance.

B. Notes, Discussion, and Open Questions

A stochastic trigger mechanism like the discussed scheme offers the advantage of reducing the communication rate significantly while keeping the required computations simple. The relationship between communication rate and error covariance is, for instance, studied in [40], [46]. The exploitation of implicit information bounds the worst-case estimation error to the case where only (13) is used for the measurement update. Without the implicit information, the remote estimator has to skip the measurement update leading to potentially unbounded errors. The bounds also allow asymptotic studies of the scheme when time-invariant models are considered and contribute to finding suitable parameters for the trigger (7). In this paper, we employ time-variant models and trigger matrices $\mathbf{Z}_k$. Although the scheme is more general with such models, we have to be aware that the sensor and the estimator have to use the same model parameters to keep the FIR estimates synchronized.

There is a wide range of possibilities to define the trigger mechanism. A simple send-on-delta scheme that sets $\underline{c}_k$ to the last transmitted measurement can be ignorant about the underlying system model. However, a more intelligent trigger design that tries to predict the course of future sensor readings is typically much more efficient but requires the sensor to understand the underlying process. The trigger can also implement a Kalman filter or receives a feedback from the remote estimator [46]. The FIR-based scheme revisited in this paper offers some advantages as compared to a Kalman filter-based scheme: First, the sensor does not need prior information about the state. Second, transmissions from remote estimator to sensor are not required. Third, the trigger design inherits the robustness to outliers from the FIR filter, which leads to lower transmission rates in the presence of unmodeled disturbances.

A disadvantage of the filter-based triggers is the required synchronization between the sensor and the remote estimator. In the discussed scheme [44], the sensor needs to transmit both $\underline{\mathbf{y}}_k$ and $\hat{\underline{\mathbf{x}}}_k^{\mathrm{FIR}}$. However, the measurement information is already encoded in the FIR estimate which renders the transmitted data redundant. Hence, we intend to redesign the trigger such that only $\hat{\underline{\mathbf{x}}}_k^{\mathrm{FIR}}$ is sent to the estimator for $\gamma_k = 1$. As a consequence, we need to adapt the remote Kalman filter such that it can incorporate the FIR estimate in the measurement update for $\gamma_k = 1$. Such a scheme will have two advantages:

1) The sensor needs to transmit less data. This is particularly advantageous for high-dimensional measurements. It is also possible to consider a multisensor system as sender in place of a single sensor. In this case, the transmission of the FIR estimate could also be more effective than sending all measurements.
2) The FIR estimate comprises also past measurements while the remote estimator in [44] only incorporates the current received measurement. Suppose that multiple transmissions have not been triggered, i.e., $\gamma_{k-1-l} = \ldots = \gamma_{k-1} = 0, l > 0$. The estimator then has only access to the implicit measurements $\hat{\underline{\mathbf{y}}}_{k-1-l}^{\mathrm{FIR}}, \ldots, \hat{\underline{\mathbf{y}}}_{k-1}^{\mathrm{FIR}}$. For $\gamma_k = 1$ at time step k, the estimator now receives the FIR estimate from the sensor. Fusing $\hat{\underline{\mathbf{x}}}_k^{\mathrm{FIR}}$ into the remote estimator should improve the estimation performance with the included information about the past measurements.

The following section describes the proposed event-based estimator exploiting the FIR-based trigger.

V. Event-Based Kalman Filtering with Correlated FIR-Estimates

The critical step of the proposed concept is the fusion of the sent FIR estimate with the remote Kalman estimate. For this purpose, we employ the Bar-Shalom–Campo fusion formulas [10] that yield optimal fusion results provided that the cross-covariance matrix is known. We determine the cross-covariance matrix by analyzing the error terms of both estimates. As a starting point, we define

$$\boldsymbol{\mathcal{U}}_k := \left(\boldsymbol{\mathcal{H}}_k^{\mathrm{T}}\,\mathbf{V}_k^{-1}\,\boldsymbol{\mathcal{H}}_k\right)^{-1}\boldsymbol{\mathcal{H}}_k^{\mathrm{T}}\,\mathbf{V}_k^{-1}$$

and

$$\boldsymbol{\mathcal{L}}_k := \begin{bmatrix} \mathbf{0}_{n_y \times n_x} & \cdots & \mathbf{0}_{n_y \times n_x} \\ \mathbf{C}_{k-1}\left(\boldsymbol{\mathcal{A}}_{k-1}^{k-1}\right)^{-1} & & \\ \vdots & \ddots & \\ \mathbf{C}_{k-m}\left(\boldsymbol{\mathcal{A}}_{k-1}^{k-m}\right)^{-1} & \cdots & \mathbf{C}_{k-m}\left(\boldsymbol{\mathcal{A}}_{k-m}^{k-m}\right)^{-1} \end{bmatrix}$$

to rewrite equation (11) as

$$\tilde{\underline{\boldsymbol{x}}}_k^{\mathrm{FIR}} = \hat{\underline{\mathbf{x}}}_k^{\mathrm{FIR}} - \underline{\mathbf{x}}_k = \boldsymbol{\mathcal{U}}_k\left(-\boldsymbol{\mathcal{L}}_k\underline{\mathbf{w}}_k^{\mathrm{last}} + \underline{\mathbf{v}}_k^{\mathrm{last}}\right) \tag{14}$$

with

$$\underline{\mathbf{w}}_k^{\mathrm{last}} := \begin{bmatrix} \underline{\mathbf{w}}_{k-1} \\ \vdots \\ \underline{\mathbf{w}}_{k-m} \end{bmatrix} \in \mathbb{R}^{m\,n_x} , \underline{\mathbf{v}}_k^{\mathrm{last}} := \begin{bmatrix} \underline{\mathbf{v}}_k \\ \vdots \\ \underline{\mathbf{v}}_{k-m} \end{bmatrix} \in \mathbb{R}^{(m+1)\,n_y} .$$

The error of the FIR estimate is a linear combination of the noise terms of the $(m+1)$ recent steps, and the FIR estimate is uncorrelated to older noise terms. Therefore, we will write the error of the Kalman estimate in terms of the $(m+1)$ recent noise terms as well. To compute the correlations with the remote Kalman filter estimate, we will bring the Kalman estimate into a similar form.

For the Kalman estimate, we introduce the matrices $\boldsymbol{\mathcal{F}}_{k|k}$ and $\boldsymbol{\mathcal{G}}_{k|k}$ and a variable $\tilde{\underline{\boldsymbol{x}}}^{\text{rest}}_{k|k}$ that represents all noise terms that are uncorrelated with the FIR estimate. These matrices are designed such that the estimation error of the Kalman filter can be represented in the form

$$\tilde{\underline{\boldsymbol{x}}}_{k|k} = \hat{\underline{\mathbf{x}}}_{k|k} - \underline{\mathbf{x}}_k = \boldsymbol{\mathcal{F}}_{k|k}\, \underline{\mathbf{w}}^{\text{last}}_k + \boldsymbol{\mathcal{G}}_{k|k}\, \underline{\mathbf{v}}^{\text{last}}_k + \tilde{\underline{\boldsymbol{x}}}^{\text{rest}}_{k|k} \quad (15)$$

resembling (14). Given the matrices $\boldsymbol{\mathcal{F}}_{k|k}$ and $\boldsymbol{\mathcal{G}}_{k|k}$, we can compute the cross-covariance matrix for $\hat{\underline{\mathbf{x}}}_{k|k}$ and $\hat{\underline{\mathbf{x}}}^{\text{FIR}}_k$, i.e.,

$$\begin{aligned}\text{Cov}[\hat{\underline{\mathbf{x}}}_{k|k}, \hat{\underline{\mathbf{x}}}^{\text{FIR}}_k] &= \mathbb{E}\left\{(\hat{\underline{\mathbf{x}}}_{k|k} - \underline{\mathbf{x}}_k)(\hat{\underline{\mathbf{x}}}^{\text{FIR}}_k - \underline{\mathbf{x}}_k)^{\text{T}}\right\} \\ &= -\boldsymbol{\mathcal{F}}_{k|k} \cdot \boldsymbol{\mathcal{Q}} \cdot \boldsymbol{\mathcal{L}}^{\text{T}}_k \boldsymbol{\mathcal{U}}^{\text{T}}_k + \boldsymbol{\mathcal{G}}_{k|k-1} \cdot \boldsymbol{\mathcal{R}} \cdot \boldsymbol{\mathcal{U}}^{\text{T}}_k . \end{aligned} \quad (16)$$

with $\boldsymbol{\mathcal{Q}} = \mathbb{E}\left\{\underline{\mathbf{w}}^{\text{last}}_k (\underline{\mathbf{w}}^{\text{last}}_k)^{\text{T}}\right\} \in \mathbb{R}^{m\, n_x \times m\, n_x}$ and $\boldsymbol{\mathcal{R}} = \mathbb{E}\left\{\underline{\mathbf{v}}^{\text{last}}_k (\underline{\mathbf{v}}^{\text{last}}_k)^{\text{T}}\right\} \in \mathbb{R}^{(m+1)\, n_z \times (m+1)\, n_z}$, which are block-diagonal matrices with $\mathbf{Q}$ and $\mathbf{R}$ as the diagonal blocks, respectively. Hence, we need to determine the matrices $\boldsymbol{\mathcal{F}}_{k|k}$ and $\boldsymbol{\mathcal{G}}_{k|k}$ in each time step k. For $k = 0$, the matrices are initialized with zero and the following subsections show how to predict and update these matrices alongside the Kalman estimate. In particular, the FIR estimate is fused with the Kalman estimate using the Bar-Shalom–Campo formulas.

A. Prediction

In this section, we describe how the prediction step of the remote Kalman filter affects the matrices $\boldsymbol{\mathcal{F}}_{k|k}$ and $\boldsymbol{\mathcal{G}}_{k|k}$. By using eq. (1) and (2), the estimation error can be written as

$$\begin{aligned}\tilde{\underline{\boldsymbol{x}}}_{k+1|k} &= \hat{\underline{\mathbf{x}}}_{k+1|k} - \underline{\mathbf{x}}_{k+1} = \mathbf{A}_k \hat{\underline{\mathbf{x}}}_{k|k} - (\mathbf{A}_k \underline{\mathbf{x}}_k + \underline{\mathbf{w}}_k) \\ &= \mathbf{A}_k \left(\hat{\underline{\mathbf{x}}}_{k|k} - \underline{\mathbf{x}}_k\right) - \underline{\mathbf{w}}_k \\ &= \mathbf{A}_k \left(\boldsymbol{\mathcal{F}}_{k|k} \underline{\mathbf{w}}^{\text{last}}_k + \boldsymbol{\mathcal{G}}_{k|k} \underline{\mathbf{v}}^{\text{last}}_k\right) + \mathbf{A}_k \tilde{\underline{\boldsymbol{x}}}^{\text{rest}}_{k+1|k} - \underline{\mathbf{w}}_k\end{aligned}$$

with (15). We intend to express this equation in terms of $\underline{\mathbf{w}}^{\text{last}}_{k+1}$ and $\underline{\mathbf{v}}^{\text{last}}_{k+1}$ to attain

$$\tilde{\underline{\boldsymbol{x}}}_{k+1|k} = \boldsymbol{\mathcal{F}}_{k+1|k}\, \underline{\mathbf{w}}^{\text{last}}_{k+1} + \boldsymbol{\mathcal{G}}_{k+1|k}\, \underline{\mathbf{v}}^{\text{last}}_{k+1} + \tilde{\underline{\boldsymbol{x}}}^{\text{rest}}_{k+1|k} . \quad (17)$$

To compute the desired matrices $\boldsymbol{\mathcal{F}}_{k+1|k}$ and $\boldsymbol{\mathcal{G}}_{k+1|k}$, we introduce the shifting matrices

$$\begin{aligned}\boldsymbol{\mathcal{N}}_w &:= \begin{bmatrix} \mathbf{0}_{n_x \times (m-1) n_x} & \mathbf{0}_{n_x} \\ \mathbf{I}_{(m-1) n_x} & \mathbf{0}_{(m-1) n_x \times n_x} \end{bmatrix} , \\ \boldsymbol{\mathcal{N}}_v &:= \begin{bmatrix} \mathbf{0}_{n_y \times m n_y} & \mathbf{0}_{n_y} \\ \mathbf{I}_{m n_y} & \mathbf{0}_{m n_y \times n_y} \end{bmatrix} .\end{aligned}$$

In doing the updated matrices become

$$\begin{aligned}\boldsymbol{\mathcal{F}}_{k+1|k} &= \mathbf{A}_k \boldsymbol{\mathcal{F}}_{k|k} \boldsymbol{\mathcal{N}}_w - \begin{bmatrix}\mathbf{I}_{n_x} & \mathbf{0}_{n_x \times (m-1) n_x}\end{bmatrix} , \\ \boldsymbol{\mathcal{G}}_{k+1|k} &= \mathbf{A}_k \boldsymbol{\mathcal{G}}_{k|k} \boldsymbol{\mathcal{N}}_v .\end{aligned}$$

The remaining term $\tilde{\underline{\boldsymbol{x}}}^{\text{rest}}_{k+1|k}$ can be computed accordingly, which now includes the error terms $\underline{\mathbf{w}}_{k-m}$ and $\underline{\mathbf{v}}_{k-m}$. The estimation error $\tilde{\underline{\boldsymbol{x}}}_{k+1|k}$ does not depend on $\underline{\mathbf{v}}_k$, which is already part of $\underline{\mathbf{v}}^{\text{last}}_{k+1}$. It will enter the error in the filtering step.

B. Filtering

Given the matrices $\boldsymbol{\mathcal{F}}_{k|k-1}$ and $\boldsymbol{\mathcal{G}}_{k|k-1}$ from the previous prediction step, the filtering step of the Kalman filter requires the computation of the updated matrices $\boldsymbol{\mathcal{F}}_{k|k}$ and $\boldsymbol{\mathcal{G}}_{k|k}$. In the event-based scheme illustrated in Fig. 1, either the remote estimator receives a new FIR estimate, or it has to resort to implicit measurement information. Depending on the triggering decision, the following update rules apply.

a) $\gamma_k = 1$: In this case, the sensor transmits the FIR estimate $\hat{\underline{\mathbf{x}}}^{\text{FIR}}_k$. The cross covariance matrix

$$\mathbf{P}^{\text{crcov}} := \text{Cov}[\hat{\underline{\mathbf{x}}}_{k|k-1}, \hat{\underline{\mathbf{x}}}^{\text{FIR}}_k] \quad (18)$$

can be computed as described earlier by equation (16). The receiver employs the Bar-Shalom–Campo formulas [10] to achieve an optimal fusion with $\hat{\underline{\mathbf{x}}}_{k|k-1}$, which yields

$$\begin{aligned}\hat{\underline{\mathbf{x}}}_{k|k} &:= (\mathbf{I}_{n_x} - \mathbf{K}^{\text{BC}}_k) \hat{\underline{\mathbf{x}}}_{k|k-1} + \mathbf{K}^{\text{BC}}_k \hat{\underline{\mathbf{x}}}^{\text{FIR}}_k \\ \mathbf{P}_{k|k} &:= \mathbf{P}_{k|k-1} - \mathbf{K}^{\text{BC}}_k (\mathbf{P}_{k|k-1} - \mathbf{P}^{\text{crcov}}) \\ \mathbf{K}^{\text{BC}}_k &:= (\mathbf{P}_{k|k-1} - \mathbf{P}^{\text{crcov}}) \cdot \\ &\qquad \left(\mathbf{P}_{k|k-1} + \mathbf{V}_k - \mathbf{P}^{\text{crcov}} - (\mathbf{P}^{\text{crcov}})^{\text{T}}\right)^{-1} .\end{aligned}$$

These computations represent the major differences to the previous scheme described in Sec. III. For the following computations, e.g., another measurement update with (18) in the subsequent time step, the matrices $\boldsymbol{\mathcal{F}}_{k|k}$ and $\boldsymbol{\mathcal{G}}_{k|k}$ need to be computed using the estimation error

$$\begin{aligned}\tilde{\underline{\boldsymbol{x}}}_{k|k} &= (\mathbf{I}_{n_x} - \mathbf{K}^{\text{BC}}_k) \hat{\underline{\mathbf{x}}}_{k|k-1} + \mathbf{K}^{\text{BC}}_k \hat{\underline{\mathbf{x}}}^{\text{FIR}}_k - \underline{\mathbf{x}}_k \\ &= (\mathbf{I}_{n_x} - \mathbf{K}^{\text{BC}}_k) \tilde{\underline{\boldsymbol{x}}}_{k|k-1} + \mathbf{K}^{\text{BC}}_k \tilde{\underline{\boldsymbol{x}}}^{\text{FIR}}_k \\ &= (\mathbf{I}_{n_x} - \mathbf{K}^{\text{BC}}_k) \left(\boldsymbol{\mathcal{F}}_{k|k-1} \underline{\mathbf{w}}^{\text{last}}_k + \boldsymbol{\mathcal{G}}_{k|k-1} \underline{\mathbf{v}}^{\text{last}}_k\right) \\ &\quad + \mathbf{K}^{\text{BC}}_k \left(-\boldsymbol{\mathcal{U}} \boldsymbol{\mathcal{L}}_k\, \underline{\mathbf{w}}^{\text{last}}_k + \boldsymbol{\mathcal{U}}_k\, \underline{\mathbf{v}}^{\text{last}}_k\right) \\ &\quad + (\mathbf{I}_{n_x} - \mathbf{K}^{\text{BC}}_k) \tilde{\underline{\boldsymbol{x}}}^{\text{rest}}_{k|k-1}\end{aligned}$$

by using (14) and (17). With this relationship, both matrices can be updated through

$$\begin{aligned}\boldsymbol{\mathcal{F}}_{k|k} &= (\mathbf{I}_{n_x} - \mathbf{K}^{\text{BC}}_k) \boldsymbol{\mathcal{F}}_{k|k-1} - \mathbf{K}^{\text{BC}}_k \boldsymbol{\mathcal{U}} \boldsymbol{\mathcal{L}} , \\ \boldsymbol{\mathcal{G}}_{k|k} &= (\mathbf{I}_{n_x} - \mathbf{K}^{\text{BC}}_k) \boldsymbol{\mathcal{G}}_{k|k-1} + \mathbf{K}^{\text{BC}}_k \boldsymbol{\mathcal{U}} ,\end{aligned}$$

which also characterize a full correlation between the Kalman estimate and the FIR estimate at the sensor as the latter has been fully incorporated into the former.

b) $\gamma_k = 0$: If no transmission is triggered at the sensor, the remote estimator exploits the implicit measurement information (12). This update is performed as described in Sec. IV, part 2) b). Also in this step, the matrices $\boldsymbol{\mathcal{F}}_{k|k-1}$ and $\boldsymbol{\mathcal{G}}_{k|k-1}$ have to be updated. The implicit measurement

$$\hat{\underline{\mathbf{y}}}^{\text{FIR}}_k = \mathbf{C}_k \underline{\mathbf{x}}_k + \underline{\mathbf{v}}_k + \underline{\mathbf{v}}^{\text{trig}}_k = \underline{\mathbf{y}}_k + \underline{\mathbf{v}}^{\text{trig}}_k$$

is related to the actual measurement $\underline{\mathbf{y}}_k$ affected by an additional independent noise $\underline{\mathbf{v}}^{\text{trig}}_k$ introduced by the stochastic trigger mechanism (13). The estimation error then becomes

$$
\begin{aligned}
\underline{\tilde{\boldsymbol{x}}}_{k|k} &= \underline{\hat{\mathbf{x}}}_{k|k-1} + \mathbf{K}_k \left(\underline{\hat{\mathbf{y}}}_k^{\mathrm{FIR}} - \mathbf{C}_k \underline{\hat{\mathbf{x}}}_{k|k-1} \right) - \underline{\mathbf{x}}_k \\
&= \underline{\tilde{\boldsymbol{x}}}_{k|k-1} + \mathbf{K}_k \left(-\mathbf{C}_k \underline{\tilde{\boldsymbol{x}}}_{k|k-1} + \underline{\mathbf{v}}_k + \underline{\mathbf{v}}_k^{\mathrm{trig}} \right) \\
&= (\mathbf{I}_{n_x} - \mathbf{K}_k \mathbf{C}_k) \underline{\tilde{\boldsymbol{x}}}_{k|k-1} + \mathbf{K}_k \underline{\mathbf{v}}_k + \mathbf{K}_k \underline{\mathbf{v}}_k^{\mathrm{trig}} \\
&= (\mathbf{I}_{n_x} - \mathbf{K}_k \mathbf{C}_k) \left(\boldsymbol{\mathcal{F}}_{k|k-1} \underline{\mathbf{w}}_k^{\mathrm{last}} + \boldsymbol{\mathcal{G}}_{k|k-1} \underline{\mathbf{v}}_k^{\mathrm{last}} \right) \\
&\quad + \mathbf{K}_k \underline{\mathbf{v}}_k + \mathbf{K}_k \underline{\mathbf{v}}_k^{\mathrm{trig}} + (\mathbf{I}_{n_x} - \mathbf{K}_k \mathbf{C}_k) \underline{\tilde{\boldsymbol{x}}}_{k|k-1}^{\mathrm{rest}} \ .
\end{aligned}
$$

The last two terms are summarized in $\underline{\tilde{\boldsymbol{x}}}_{k|k}^{\mathrm{rest}}$. As a result, we can infer the following update equations

$$
\begin{aligned}
\boldsymbol{\mathcal{F}}_{k|k} &= (\mathbf{I}_{n_x} - \mathbf{K}_k \mathbf{C}_k) \boldsymbol{\mathcal{F}}_{k|k-1} \ , \\
\boldsymbol{\mathcal{G}}_{k|k} &= (\mathbf{I}_{n_x} - \mathbf{K}_k \mathbf{C}_k) \boldsymbol{\mathcal{G}}_{k|k-1} + \begin{bmatrix} \mathbf{K}_k & \mathbf{0}_{n_y \times m n_y} \end{bmatrix} \ .
\end{aligned}
$$

C. Summary

Compared to the approach in [44], the proposed scheme requires adaptions at the remote estimator. The prediction and filtering step of the Kalman filter are now accompanied by the computation of the matrices $\boldsymbol{\mathcal{F}}_{k|k}$ and $\boldsymbol{\mathcal{G}}_{k|k}$. Also, $\boldsymbol{\mathcal{U}}_k$ and $\boldsymbol{\mathcal{L}}_k$ need to be computed for the cross-covariance matrix in (18) when a transmission has been triggered. However, this computational overhead at the receiver rewards us with a lower amount of data to be transmitted and a better estimation quality. The latter can in particular be seen when low communication rates are aspired, which is demonstrated in the following.

VI. Simulation

In this section, we study Monte-Carlo simulations to evaluate the proposed scheme, which is abbreviated by FusionFIR in the following. For each time step k, we simulate a state $\underline{\mathbf{x}}_k$. State transitions and measurements are done as described in section III-A, a simulation run consists of 100 time steps.

The simulation consists of a sensor and a remote state estimator. The sensor employs the FIR-based trigger mechanism as described in IV-A1. With the abbreviation KFFIR, we denote the concept that employs a remote estimator as described in IV-A2, which is the solution from [44]. We use the mean squared error (MSE) over $5{,}000$ runs to compare the performance of FusionFIR and KFFIR. The process noise $\underline{\mathbf{w}}_k$, the measurement noise $\underline{\mathbf{v}}_k$ and the trigger noise $\boldsymbol{\xi}_k$ are generated for each run and step independently.

We choose a two-dimensional *nearly-constant-velocity model* as a basis for our evaluation. The state is given by $\underline{\mathbf{x}} := \begin{bmatrix} p_x & v_x & p_y & v_y \end{bmatrix}^\top$, and the position is measured by a remote sensor. The system and sensor models are characterized by the following matrices

$$
\mathbf{A}_k = \begin{bmatrix} 1 & \Delta & 0 & 0 \\ 0 & 1 & 0 & 0 \\ 0 & 0 & 1 & \Delta \\ 0 & 0 & 0 & 1 \end{bmatrix} , \qquad \mathbf{C}_k = \begin{bmatrix} 1 & 0 & 0 & 0 \\ 0 & 0 & 1 & 0 \end{bmatrix} ,
$$

$$
\mathbf{Q}_k = q \cdot \begin{bmatrix} \Delta^3/3 & \Delta^2/2 & 0 & 0 \\ \Delta^2/2 & \Delta & 0 & 0 \\ 0 & 0 & \Delta^3/3 & \Delta^2/2 \\ 0 & 0 & \Delta^2/2 & \Delta \end{bmatrix} , \quad \mathbf{R}_k = \begin{bmatrix} 1 & 0 \\ 0 & 1 \end{bmatrix} ,
$$

where $\Delta = 0.1$ is the sampling interval, and q is a power spectral density. Initially, we set $q = 0.1$. The horizon for the FIR estimate is set to $m = 4$. We control the communication rate via a scalar z by setting $\mathbf{Z} = z \cdot \mathbf{I}_2$. To get an initial $\underline{\hat{\mathbf{x}}}_0^{\mathrm{FIR}}$ at the sensor, we simulate at least m previous time steps. All measurements before time step $k = 0$ are transmitted, and each scheme uses a standard Kalman filter to incorporate them optimally. In doing so, each scheme has access to the same information at the time step $k = 0$ to ensure a fair comparison. For this purpose, we set $\mathbf{P}_{-m} = 10 \cdot \mathbf{I}_4, \underline{\hat{\mathbf{x}}}_{-m} = \underline{0}$ and sample $\underline{\mathbf{x}}_{-m} \sim \mathcal{N}(\underline{0}, \mathbf{P}_{-m})$ for each run.

Fig. 2.a) shows the results depending on the communication rate. For communication rates below 50%, the differences become clearly visible, and the estimations made by FusionFIR are far better than the estimations made with KFFIR. The figures also include a lower bound, for which we assume that the sensor just sends all measurements acquired between triggering events, and the optimal remote Kalman estimate is then computed given all received measurements. We see that FusionFIR is close to that lower bound. We compare the approaches more deeply by the following variations.

1) Impact of communication rates around 100 %: Fig. 2.a) also shows that FusionFIR may perform slightly worse than KFFIR for communication rates around 100%. The explanation of this phenomenon is the nature of the optimality of the Bar-Shalom–Campo fusion formulas; the fusion formulas are only optimal in an ML sense but not in an MMSE sense [11]. Since KFFIR is for a communication rate of 100% identical to a standard Kalman filter and thus optimal in an MMSE sense. This case can outperform the fusion with an FIR estimate.

2) Impact of the horizon $m+1$: In Fig. 2.a), the results of FusionFIR and the lower bound are close. This means that the FIR estimates $\underline{\hat{\mathbf{x}}}_k^{\mathrm{FIR}}$ sent by the sensor do carry a similar amount of information like an optimal Kalman estimate. This indicates that the measurements which are considered by the Kalman estimate but not by the FIR estimate are of little value, which raises the question of whether this is also true for smaller horizons. We, therefore, reduce the horizon to 3, i.e., $m = 2$.

The results are shown in Fig. 2.b). The plots of FusionFIR and the lower bound are now slightly more apart. This is expected because an FIR estimate with a smaller horizon is lacking information. However, the smaller horizon also changes the sensor's trigger decisions: These directly depend on the quality of the FIR state estimates. Therefore, reducing the horizon also makes trigger decisions more likely. This is also visible in Fig. 2.b). Compared to Fig. 2.a) (with the exception of 100% communication rate) the plot is shifted to the right side, meaning that for the same values of the matrix $\mathbf{Z}$, a trigger decision is more likely with a reduced horizon. For example, communication rates around 40% lead to an MSE for all methods below 2 if $m = 4$. The MSE increases to 2 and higher if the horizon is reduced to 3, i.e., $m = 2$.

3) Impact of the system noise: Compared to the measurement noise, the system noise of the chosen system is small. We have increased the system noise by a factor 10 to see the impact of the system noise. Fig. 2.c) shows the results. The gap in estimation quality between FusionFIR and KFFIR shrinks. Also, the gap between the lower bound and FusionFIR is now

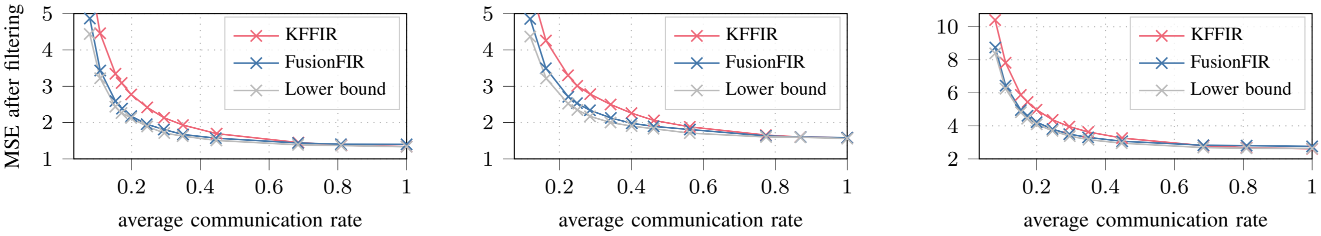

(a) $m = 4$, $q = 0.1$, $\Delta = 0.1$ (b) $m = 2$, $q = 0.1$, $\Delta = 0.1$ (c) $m = 4$, $q = 1$, $\Delta = 0.1$

Fig. 2: MSE over average communication rate for the constant velocity system. Each dot represent the average result over 5000 runs of our simulation with 100 time steps each.

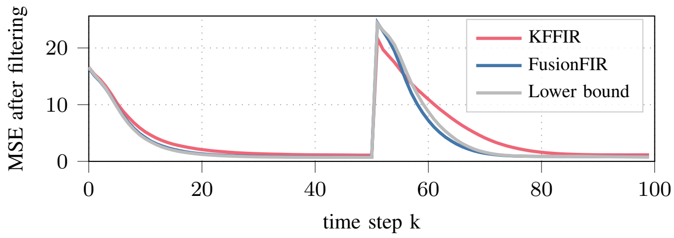

Fig. 3: MSE over time with $q = 0.1, \Delta = 0.1, m = 4$ and $\mathbf{Z} = 10 \cdot \mathbf{I}_2$. An unmodeled impulse is applied after 50 steps.

reduced. A higher process noise implies that the information gain by processing old measurements is reduced.

4) Impact of initial and temporary unmodeled errors: We want to conclude our evaluation by analyzing the impact of initial and temporary unmodeled errors. We introduce such temporary unmodeled errors by setting $\underline{\mathbf{x}}_{51}$ to $\mathbf{A}_{50} \cdot \underline{\mathbf{x}}_{50} + \underline{\mathbf{w}}_{50} + 2.5 \cdot \underline{1}$, which means we add an impulse to the state prediction. The trigger and estimator are ignorant about this error. We use the parameters $q = 0.1, \Delta = 0.1, m = 4$ and $\mathbf{Z} = 10 \cdot \mathbf{I}_2$, which yields an average communication rate of 25%. We compute the MSE for each time step k and also increase the number of runs to $50\,000$.

The results are illustrated in Fig. 3. FusionFIR recovers from the initialization error faster and converges to a lower MSE than KFFIR. The performance of FusionFIR is similar to the lower bound method. This is expected and goes along with Fig. 2.a). Applying an unmodeled impulse causes different reactions: Directly after application, the MSE is lower if KFFIR is used, but FusionFIR and the lower bound algorithm recover from the temporary error much faster and FusionFIR is better than KFFIR after a few steps. Both effects are due to the processing of old measurements. The FusionFIR algorithm incorporates older measurements. The application of the impulse renders these old measurements useless, because the impulse is unmodeled. Therefore, the FusionFIR still includes the outlier over a horizon and leads to higher MSE, and KFFIR performs better directly after application of the impulse. However, after some steps, the FIR estimate does only contain measurements obtained after the impulse, FusionFIR then outperforms the KFFIR method. It may even recover faster than the lower bound, which is essentially an optimal Kalman filter incorporating delayed measurements. This reflects that an FIR filter is less affected by temporary unmodeled errors than a Kalman filter, making the FIR-based trigger mechanism attractive.

VII. Conclusions

Using an FIR-based stochastic trigger offers several beneficial properties like resilience to unmodeled disturbances, a simple initialization, and high estimation quality paired with a low communication rate. Despite the additional computation of the FIR estimate at the sensor, the formulation in [44] requires the sensor to transmit both the sensor data and the FIR estimate when an event is triggered. The remote Kalman filter uses the former for the measurement update and the latter to deduce implicit information in future time steps. With this paper, the sensor only needs to transmit the FIR estimate so that less data is transmitted rendering this scheme particularly useful for high-dimensional sensor data. The measurement update for $\gamma_k = 1$ is replaced by an optimal fusion with the received FIR estimate exploiting the cross-covariances. In doing so, the quality of the remote estimate is further improved as the FIR estimate incorporates past measurements which is a second major advantage of this approach and has been demonstrated in the simulations. A drawback of the proposed scheme can be additional resource requirements for the computation and bookkeeping of the cross-covariance matrices needed for fusion.

Future directions include the extension to multisensor systems as well as other trigger mechanisms that require adapted fusion formulas. Also, a promising research question is whether further improvements to the remote estimate are possible as the optimal fusion does not yield the optimal estimate given all measurements [11]. Another challenge to be addressed are unreliable communication channels affected by packet delays and drops [47]. In this case, the remote estimate cannot discern whether the trigger or other effects account for the absence of a transmission.

References

[1] W. Dargie and C. Poellabauer, *Fundamentals of Wireless Sensor Networks*. John Wiley & Sons, Oct. 2010.

[2] J. Nygårds, V. Deleskog, and G. Hendeby, "Decentralized Tracking in Sensor Networks with Varying Coverage," in *Proc. of the 21st Int. Conference on Information Fusion (Fusion 2018)*, Cambridge, United Kingdom, Jul. 2018.

[3] R. Dautov and S. Distefano, "Distributed Data Fusion for the Internet of Things," in *Lecture Notes in Computer Science*. Springer Int. Publishing, 2017, pp. 427–432.

[4] W. Wu, Z. Yang, and K. Li, "Internet of Vehicles and Applications," in *Internet of Things*. Elsevier, 2016, pp. 299–317.

[5] J. Liu, H. Shen, H. S. Narman, W. Chung, and Z. Lin, "A Survey of Mobile Crowdsensing Techniques," *ACM Trans. on Cyber-Physical Systems*, vol. 2, no. 3, pp. 1–26, jul 2018.

[6] D. L. Hall, C.-Y. Chong, J. Llinas, and M. E. Liggins II, Eds., *Distributed Data Fusion for Network-Centric Operations*, ser. The Electrical Engineering and Applied Signal Processing Series. CRC Press, 2013.

[7] B. Noack, *State Estimation for Distributed Systems with Stochastic and Set-membership Uncertainties*, ser. Karlsruhe Ser. on Intelligent Sensor-Actuator-Systems 14. Karlsruhe, Germany: KIT Scient. Publ., 2013.

[8] M. E. Campbell and N. R. Ahmed, "Distributed Data Fusion: Neighbors, Rumors, and the Art of Collective Knowledge," *IEEE Control Systems Magazine*, vol. 36, no. 4, pp. 83–109, Aug. 2016.

[9] B. Noack, J. Sijs, M. Reinhardt, and U. D. Hanebeck, "Treatment of Dependent Information in Multisensor Kalman Filtering and Data Fusion," in *Multisensor Data Fusion: From Algorithms and Architectural Design to Applications*, H. Fourati, Ed. CRC Press, Aug. 2015, pp. 169–192.

[10] Y. Bar-Shalom and L. Campo, "The Effect of the Common Process Noise on the Two-Sensor Fused-Track Covariance," *IEEE Trans. on Aerospace and Electronic Systems*, vol. 22, no. 6, pp. 803–805, Nov. 1986.

[11] K.-C. Chang, R. K. Saha, and Y. Bar-Shalom, "On Optimal Track-to-Track Fusion," *IEEE Trans. on Aerospace and Electronic Systems*, vol. 33, no. 4, pp. 1271–1276, Oct. 1997.

[12] W. Koch, "On Optimal Distributed Kalman Filtering and Retrodiction at Arbitrary Communication Rates for Maneuvering Targets," in *Proc. of the 2008 IEEE Int. Conf. on Multisensor Fusion and Integration for Intelligent Systems (MFI 2008)*, Seoul, Republic of Korea, Aug. 2008.

[13] F. Govaers and W. Koch, "An Exact Solution to Track-to-track Fusion at Arbitrary Communication Rates," *IEEE Trans. on Aerospace and Electronic Systems*, vol. 48, no. 3, Jul. 2012.

[14] C.-Y. Chong, S. Mori, F. Govaers, and W. Koch, "Comparison of Tracklet Fusion and Distributed Kalman Filter for Track Fusion," in *Proc. of the 17th Int. Conf. on Information Fusion (Fusion 2014)*, Salamanca, Spain, Jul. 2014.

[15] M. Reinhardt, B. Noack, S. Kulkarni, and U. D. Hanebeck, "Distributed Kalman Filtering in the Presence of Packet Delays and Losses," in *Proc. of the 17th Int. Conf. on Information Fusion (Fusion 2014)*, Salamanca, Spain, Jul. 2014.

[16] F. Pfaff, B. Noack, U. D. Hanebeck, F. Govaers, and W. Koch, "Information Form Distributed Kalman Filtering (IDKF) with Explicit Inputs," in *Proc. of the 20th Int. Conf. on Information Fusion (Fusion 2017)*, Xi'an, China, Jul. 2017.

[17] J. Steinbring, B. Noack, M. Reinhardt, and U. D. Hanebeck, "Optimal Sample-Based Fusion for Distributed State Estimation," in *Proc. of the 19th Int. Conf. on Information Fusion (Fusion 2016)*, Heidelberg, Germany, Jul. 2016.

[18] S. Radtke, B. Noack, and U. D. Hanebeck, "Fully Decentralized Estimation Using Square-Root Decompositions," *Journ. of Advances in Information Fusion*, vol. 16, no. 1, pp. 3–16, Jun. 2021.

[19] S. J. Julier and J. K. Uhlmann, "A Non-divergent Estimation Algorithm in the Presence of Unknown Correlations," in *Proc. of the IEEE American Control Conf. (ACC 1997)*, vol. 4, Albuquerque, NM, USA, Jun. 1997.

[20] M. Reinhardt, B. Noack, P. O. Arambel, and U. D. Hanebeck, "Minimum Covariance Bounds for the Fusion under Unknown Correlations," *IEEE Signal Processing Letters*, vol. 22, no. 9, pp. 1210 – 1214, Sep. 2015.

[21] B. Noack, J. Sijs, M. Reinhardt, and U. D. Hanebeck, "Decentralized Data Fusion with Inverse Covariance Intersection," *Automatica*, vol. 79, pp. 35–41, May 2017.

[22] N. R. Ahmed, W. W. Whitacre, S. Moon, and E. W. Frew, "Factorized Covariance Intersection for Scalable Partial State Decentralized Data Fusion," in *Proc. of the 19th Int. Conf. on Information Fusion (Fusion 2016)*, Heidelberg, Germany, Jul. 2016.

[23] B. Noack, U. Orguner, and U. D. Hanebeck, "Nonlinear Decentralized Data Fusion with Generalized Inverse Covariance Intersection," in *Proc. of the 22nd Int. Conf. on Information Fusion (Fusion 2019)*, Ottawa, Canada, Jul. 2019.

[24] C. Funk, B. Noack, and U. D. Hanebeck, "Conservative Quantization of Fast Covariance Intersection," in *Proc. of the 2020 IEEE Int. Conf. on Multisensor Fusion and Integration for Intelligent Systems (MFI 2020)*, Virtual, Sep. 2020.

[25] C. Funk, B. Noack, and U. D. Hanebeck, "Conservative Quantization of Covariance Matrices with Applications to Decentralized Information Fusion," *Sensors*, vol. 21, no. 9, Apr. 2021.

[26] R. Forsling, "Decentralized Estimation Using Conservative Information Extraction," Licentiate Thesis, Linköping University, Department of Electrical Engineering, Automatic Control, Jan. 2020.

[27] G. Battistelli, A. Benavoli, and L. Chisci, "Data-driven Communication for State Estimation with Sensor Networks," *Automatica*, vol. 48, no. 5, pp. 926–935, May 2012.

[28] K. Dormann, B. Noack, and U. D. Hanebeck, "Optimally Distributed Kalman Filtering with Data-Driven Communication," *Sensors*, vol. 18, no. 4, Apr. 2018.

[29] X. Bian, X. R. Li, and V. P. Jilkov, "Remote State Estimation with Data-driven Communication and Guaranteed Stability," in *Proc. 21st Int. Conf. on Inform. Fusion (Fusion 2018)*, Cambridge, UK, Jul. 2018.

[30] F. Rosenthal, B. Noack, and U. D. Hanebeck, "Scheduling of Measurement Transmission in Networked Control Systems Subject to Communication Constraints," in *Proc. of the 2018 American Control Conf. (ACC 2018)*, Milwaukee, WI, USA, Jun. 2018.

[31] F. Rosenthal, B. Noack, and U. D. Hanebeck, "State Estimation in Networked Control Systems with Delayed and Lossy Acknowledgments," in *Multisensor Fusion and Integration in the Wake of Big Data, Deep Learning and Cyber Physical System*, S. Lee, H. Ko, and S. Oh, Eds. Cham: Springer Int. Publishing, Jul. 2018, pp. 22–38.

[32] S. Trimpe and R. D'Andrea, "Event-Based State Estimation with Variance-Based Triggering," *IEEE Trans. on Autom. Control*, vol. 59, no. 12, pp. 3266–3281, Dec. 2014.

[33] M. Muehlebach and S. Trimpe, "Distributed Event-Based State Estimation for Networked Systems: An LMI Approach," *IEEE Trans. on Automatic Control*, vol. 63, no. 1, pp. 269–276, Jan. 2018.

[34] J. Sijs, B. Noack, and U. D. Hanebeck, "Event-Based State Estimation with Negative Information," in *Proc. of the 16th Int. Conf. on Information Fusion (Fusion 2013)*, Istanbul, Turkey, Jul. 2013.

[35] J. Sijs, L. Kester, and B. Noack, "A Study on Event Triggering Criteria for Estimation," in *Proc. of the 17th Int. Conf. on Information Fusion (Fusion 2014)*, Salamanca, Spain, Jul. 2014.

[36] J. Sijs, B. Noack, M. Lazar, and U. D. Hanebeck, "Time-Periodic State Estimation with Event-Based Measurement Updates," in *Event-Based Control and Signal Processing*, M. Miskowicz, Ed. CRC Press, Nov. 2015, pp. 261–279.

[37] D. Shi, L. Shi, and T. Chen, *Event-Based State Estimation: A Stochastic Perspective*, ser. Studies in Systems, Decision and Control. Cham: Springer Int. Publishing, 2016, vol. 41.

[38] J. Sijs and B. Noack, "Event-Based Estimation in a Feedback Loop Anticipating on Imperfect Communication," in *Proc. of the 20th IFAC World Congress (IFAC 2017)*, Toulouse, France, Jul. 2017.

[39] B. Noack, F. Pfaff, and U. D. Hanebeck, "Optimal Kalman Gains for Combined Stochastic and Set-Membership State Estimation," in *Proc. of the 51st IEEE Conf. on Decision and Control (CDC 2012)*, Maui, HI, USA, Dec. 2012.

[40] M. T. Andrén and A. Cervin, "Event-Based State Estimation Using an Improved Stochastic Send-on-Delta Sampling Scheme," in *Proc. 2016 2nd Int. Conf. on Event-based Control, Communication, and Signal Processing (EBCCSP 2016)*, Krakow, Poland, Jun. 2016.

[41] A. Mohammadi and K. N. Plataniotis, "Event-Based Estimation With Information-Based Triggering and Adaptive Update," *IEEE Trans. on Signal Processing*, vol. 65, no. 18, pp. 4924–4939, Sep. 2017.

[42] J. Qian, P. Duan, and Z. Duan, "Fully Distributed Filtering with a Stochastic Event-Triggered Mechanism," *IEEE Trans. on Control of Network Systems*, 2021.

[43] B. Noack, C. Funk, S. Radtke, and U. D. Hanebeck, "State Estimation with Event-Based Inputs Using Stochastic Triggers," in *Proc. of the 21st IFAC World Congress (IFAC 2020)*, Berlin, Germany, Jul. 2020.

[44] E. J. Schmitt, B. Noack, W. Krippner, and U. D. Hanebeck, "Gaussianity-Preserving Event-Based State Estimation with an FIR-Based Stochastic Trigger," *IEEE Control Systems Letters*, vol. 3, no. 3, pp. 769–774, Jul. 2019.

[45] Y. S. Shmaliy, S. Zhao, and C. K. Ahn, "Unbiased Finite Impluse Response Filtering: An Iterative Alternative to Kalman Filtering Ignoring Noise and Initial Conditions," *IEEE Control Systems*, vol. 37, no. 5, pp. 70–89, Oct. 2017.

[46] D. Han, Y. Mo, J. Wu, S. Weerakkody, B. Sinopoli, and L. Shi, "Stochastic Event-Triggered Sensor Schedule for Remote State Estimation," *IEEE Trans. on Autom. Control*, vol. 60, no. 10, pp. 2661–2675, Oct. 2015.

[47] E. Kung, J. Wu, D. Shi, and L. Shi, "On the Nonexistence of Event-Based Triggers That Preserve Gaussian State in Presence of Package-Drop," in *Proc. 2017 Amer. Control Conf. (ACC 2017)*, Seattle, WA, USA, May 2017.